

# Dynein Intermediate Chain Mediated Dynein–Dynactin Interaction Is Required for Interphase Microtubule Organization and Centrosome Replication and Separation in *Dictyostelium*

Shuo Ma,\* Leda Triviños-Lagos,\* Ralph Gräf,<sup>‡</sup> and Rex L. Chisholm\*

\*Department of Cell and Molecular Biology, and Robert H. Lurie Comprehensive Cancer Center, Northwestern University Medical School, Chicago, Illinois 60611; and <sup>‡</sup>Adolf-Butenandt-Institut/Zellbiologie, Universitaet Muenchen, D-80336 Muenchen, Germany

**Abstract.** Cytoplasmic dynein intermediate chain (IC) mediates dynein–dynactin interaction in vitro (Karki, S., and E.L. Holzbaur. 1995. *J. Biol. Chem.* 270:28806–28811; Vaughan, K.T., and R.B. Vallee. 1995. *J. Cell Biol.* 131:1507–1516). To investigate the physiological role of IC and dynein–dynactin interaction, we expressed IC truncations in wild-type *Dictyostelium* cells. ICΔC associated with dynactin but not with dynein heavy chain, whereas ICΔN truncations bound to dynein but bound dynactin poorly. Both mutations resulted in abnormal localization to the Golgi complex, confirming dynein function was disrupted. Striking disorganization of interphase microtubule (MT) networks was observed when mutant expression was induced. In a majority of cells, the MT networks collapsed into large bundles. We also observed cells with multiple cytoplasmic asters and MTs lacking an organizing center.

These cells accumulated abnormal DNA content, suggesting a defect in mitosis. Striking defects in centrosome morphology were also observed in IC mutants, mostly larger than normal centrosomes. Ultrastructural analysis of centrosomes in IC mutants showed interphase accumulation of large centrosomes typical of prophase as well as unusually paired centrosomes, suggesting defects in centrosome replication and separation. These results suggest that dynactin-mediated cytoplasmic dynein function is required for the proper organization of interphase MT network as well as centrosome replication and separation in *Dictyostelium*.

**Key words:** dynein function • intermediate chain • dynein–dynactin interaction • microtubule organization • centrosome replication and separation

CYTOPLASMIC dynein, a minus-end-directed, microtubule (MT)<sup>1</sup>-based motor, has been implicated in a broad range of MT-dependent activities both in mitosis and interphase. Cytoplasmic dynein is important for spindle orientation in yeast (Eshel et al., 1993) and nuclear migration in filamentous fungi (Plamann et al., 1994; Xiang et al., 1994). In *Drosophila* and mammalian cells, it is required for spindle formation and function (Vaisberg et al., 1993; Echeverri et al., 1996; Gepner et al., 1996). During interphase, cytoplasmic dynein mediates the movement of membranous vesicles such as perinuclear positioning of the Golgi apparatus (Corthesy-Theulaz et al., 1992; Burkhardt et al., 1997; Harada et al., 1998), ER-to-Golgi

transport (Presley et al., 1997), and retrograde axonal transport (Dillman et al., 1996; Waterman-Storer et al., 1997). Despite this we have a limited understanding of how dynein is targeted and regulated to accomplish these varied functions.

The best candidate for targeting and regulating dynein activity is the dynactin complex. Dynactin, named for dynein activator, was initially isolated as a factor required to activate dynein-dependent vesicle transport in vitro (Gill et al., 1991; Schroer and Sheetz, 1991). Dynactin is a large complex containing at least nine different subunits, including p150/Glued, p50 (dynamitin), Arp1, actin, capping protein, p62, p24, and others (Schafer et al., 1994). Genetic analysis in several different organisms indicates that dynactin functions in the same genetic pathway as dynein (Clark and Meyer, 1994; Muhua et al., 1994; Plamann et al., 1994; McGrail et al., 1995; Bruno et al., 1996; Tinsley et al., 1996). Overexpression of the p50/dynamitin subunits in mammalian cells disrupted dynactin and led to dynein redistribution. These cells accumulated in prometaphase and had dispersed Golgi apparatus (Echeverri et al., 1996;

Address correspondence to Rex L. Chisholm, Department of Cell and Molecular Biology, Northwestern University Medical School, 303 East Chicago Ave., Ward 11-100, Chicago, IL 60611-3072. Tel.: (312) 503-4151. Fax: (312) 503-5994. E-mail: r-chisholm@nwu.edu

1. *Abbreviations used in this paper:* DAPI, 4,6-diamidino-2-phenylindole; HC, heavy chain; IC, intermediate chain; IP, immunoprecipitation; MT, microtubule; MTOC, MT organizing center.

Burkhardt et al., 1997). Therefore, dynactin seems important for the proper targeting and function of cytoplasmic dynein.

Among dynein subunits, the intermediate chain (IC) is an attractive candidate for regulating dynein function. Residing at the base of the dynein complex (Steffen et al., 1996), the IC is predicted to target dynein to its intracellular cargo (Paschal et al., 1992). Indeed, *in vitro* studies have shown that IC mediates the interaction between dynein and dynactin through physical association with the p150/Glued subunit of dynactin (Karki and Holzbaaur, 1995; Vaughan and Vallee, 1995). However, the direct interaction between dynein and dynactin complexes has yet to be demonstrated *in vivo*.

To investigate the *in vivo* function of cytoplasmic dynein, we overexpressed IC truncation mutants in wild-type *Dictyostelium* cells. NH<sub>2</sub>-terminal deletions bound dynein but bound dynactin poorly, whereas a COOH-terminal deletion associated with dynactin but failed to bind dynein. Although these two types of mutants interfered with endogenous IC function in a complementary way, they produced similar abnormal phenotypes, including dispersion of the Golgi complex, disruption of the interphase MT network, accumulation of abnormal DNA content, and centrosome abnormalities. Our results provide direct *in vivo* support for the role of IC as a link between dynein and dynactin as well as for the idea that this interaction may generally be required for dynein function. In addition, dynein function appears to be required for normal organization of the interphase MT network as well as centrosome replication and separation.

## Materials and Methods

### *Dictyostelium* Dynein Antibodies

*Dictyostelium*-specific dynein antibodies used were: M4, a mouse polyclonal antibody against dynein IC; IC144, a rat polyclonal antibody against IC; and NW127, a rabbit polyclonal antibody against dynein heavy chain (HC). Antibody generation will be described in Results.

### Cloning of Cytoplasmic Dynein IC from *Dictyostelium*

M4 polyclonal antibody was used to screen a  $\lambda$ gt11 cDNA expression library made from *Dictyostelium* cells developed for 4 h (Clontech Laboratories, Inc.). 10 immunoreactive phage clones were isolated, 3 of which were positive by epitope selection. The longest of these, IC10, had an open reading frame of 1,956 nucleotides. The other two clones were partial sequences contained within the IC10 sequence (sequence data available from EMBL/GenBank/DBJ under accession no. U25116).

### Expression Constructs and Transformation of *Dictyostelium* Cells

The full-length clone IC10 was used as a PCR template to amplify various IC truncation mutants. 33-nucleotide extensions were added to the 3' PCR primers (5'-TTA TAA ATC TTC TTC ACT AAT TAA TTT TTC TTC-3') to produce the COOH-terminal myc epitope tags. BamHI sites were added at the 5' ends of all PCR primers to facilitate subsequent cloning. PCR products were cloned into the BamHI site of pVEII (Blusch et al., 1992), downstream of a discoidin I- $\gamma$  promoter, whose activity can be repressed by including folate in the medium and induced by withdrawing folate.

AX3 wild-type *Dictyostelium* cells were transformed by electroporation with 10  $\mu$ g plasmid DNA as described previously (Howard et al., 1988). Transformants were cloned in 96-well plates in HL5 medium with 50  $\mu$ g/ml G418. Folate (1 mM) was added to the medium during selection and ex-

pansion of the clones. Several independent clones of each class were analyzed in each experiment to control for possible mutations caused by clonal variation.

### Immunoprecipitations and Western Blots

For immunoprecipitations (IPs),  $4 \times 10^7$  cells were collected and washed twice with 15 mM Na-KPO<sub>4</sub> buffer, pH 6.5. After resuspension in 1 ml IP buffer (50 mM Pipes, pH 6.8, 5 mM EDTA, 100 mM NaF, 25 mM Na pyrophosphate, 2.5 mM DTT, 1 mM PMSF, 50  $\mu$ g/ml leupeptin, 50  $\mu$ g/ml pepstatin, 1 mM ATP) cells were lysed by sonication. The cell lysate was cleared by centrifugation at 38,000 *g* for 30 min at 2°C. Protein A-Sepharose preincubated with the IP antibody was added to the cell lysate and the mixture incubated with rocking for at least 2 h at 4°C. Dynein HC antibody NW127 was used to immunoprecipitate dynein complex, whereas affinity-purified capping protein  $\beta$  antibody R18 (a generous gift from Dr. John Cooper, Washington University, St. Louis, MO) was used to immunoprecipitate the dynactin complex. Sepharose bead-bound immune complexes were collected by centrifugation and washed four times with IP buffer. The final pellets were resuspended in 30  $\mu$ l 2 $\times$  SDS sample buffer (125 mM Tris, pH 6.8, 4% SDS, 10% 2-mercaptoethanol, 20% glycerol), boiled for 5 min, centrifuged, and the supernatant collected. For Western blots, samples were separated on 7.5% polyacrylamide gels and transferred to polyvinylidene difluoride membranes. Blots were blocked in 5% nonfat milk and incubated with primary antibody followed by HRP-conjugated secondary antibody. Blots were developed in Renaissance enhanced chemiluminescence reagent (NEN Life Science Products) and exposed to X-ray film.

### Sucrose Density Gradient Centrifugation

For each gradient,  $2 \times 10^8$  cells were washed twice with 15 mM Na-KPO<sub>4</sub> buffer, pH 6.5, resuspended in 0.4 ml of lysis buffer (100 mM Pipes, pH 6.8, 1 mM EDTA, 5 mM EGTA, 5 mM MgSO<sub>4</sub>, 2.5 mM DTT, 1 mM PMSF, 50  $\mu$ g/ml leupeptin, 50  $\mu$ g/ml pepstatin) and lysed by sonication. After centrifugation at 38,000 *g* for 30 min at 2°C, the lysates were loaded on an 11-ml 5–20% continuous sucrose density gradient made in lysis buffer without protease inhibitors. The gradients were centrifuged in a SW41 rotor (Beckman Instruments Inc.) at 31,500 rpm for 16 h (4°C). Fractions (0.8 ml) were collected from the bottom of the gradient and protein samples prepared for Western blot analysis.

### Indirect Immunofluorescence

Cells grown on sterile coverslips were fixed and indirect immunofluorescence performed with various antibodies followed by 4,6-diamidino-2-phenylindole (DAPI) staining. To stain the Golgi complex, cells were fixed in –15°C methanol for 5 min and stained with a comitin mAb (a gift from Dr. Angelika A. Noegel, University of Cologne, Cologne, Germany). For tubulin staining, cells were fixed in 1.85% formaldehyde in 15 mM Na-KPO<sub>4</sub>, pH 6.5, for 5 min at room temperature, then extracted in –15°C methanol for 5 min, and stained with a rat anti- $\alpha$ -tubulin mAb (Serotech, Ltd.). For centrosome staining, cells were fixed with either of the two methods described above and stained with polyclonal  $\gamma$ -tubulin antibody and several different mAbs specific for *Dictyostelium* centrosomes (NAB350, 4/148, and 2/165) (Graf et al., 1999).

### Light Microscopy

Conventional immunofluorescence microscopy was carried out on an Axioskop microscope (Carl Zeiss, Inc.) equipped with a 100 $\times$ , 1.4 NA oil immersion objective. Images were taken with a cooled CCD camera (Hamamatsu Photonic Systems) controlled by MetaMorph 3.6 imaging system (Universal Imaging Corp.) and were processed with MetaMorph and Adobe Photoshop 5.0 (Adobe Systems, Inc.).

### Flow Cytometry Analysis

*Dictyostelium* cells were washed in 15 mM Na-K PO<sub>4</sub> buffer, fixed in ice-cold 70% ethanol, and stained with 50  $\mu$ g/ml propidium iodide. RNase was included in the staining solution to remove double-stranded RNA. The nuclear DNA content of the stained samples was analyzed using FACS-Calibur (Beckton Dickinson).

### Electron Microscopy

Cells grown on coverslips were fixed in 4% glutaraldehyde in 0.1 M So-

rensens phosphate buffer, pH 7.4, rinsed, and postfixed in 1% osmium tetroxide in 0.1 M Sorensens phosphate buffer, pH 7.4 for 1 h. After dehydration in ethanol and propylene oxide, they were embedded in POLY/BED 812 (Polysciences Inc.). After polymerization at 60°C for 48 h, coverslips were removed, and serial sections were cut about 90-nm thick on a Reichert-Jung Ultracut E ultramicrotome (Leica, Inc.). After staining in 4% uranyl acetate followed by Reynolds lead, sections were viewed and photographed on a JEOL JEM 1220 transmission electron microscope at 15,000 $\times$  to 40,000 $\times$  magnification.

## Results

### Cloning of the *Dictyostelium* Dynein IC

Cytoplasmic dynein was isolated from vegetatively growing *Dictyostelium* cells (Koonce and McIntosh, 1990). *Dictyostelium* dynein contains a 530-kD dynein HC, an 83-kD IC, and a 58-kD light IC (Fig. 1, lane 2). The 83-kD IC, purified from SDS-PAGE gels, was used to generate polyclonal antisera in mice. One of these antisera, M4, reacted specifically with an 83-kD protein on Western blots of *Dictyostelium* whole cell extract and with the IC of purified dynein (Fig. 1, lanes 3–4). M4 was used to screen a *Dictyostelium* cDNA expression library. A full-length clone, IC10, encodes a protein of 651-amino acids, predicted to have an  $M_r$  of 72 kD. For subsequent experiments, we generated additional *Dictyostelium* dynein antibodies: polyclonal rat antibody IC144 was raised against bacterially expressed IC (Fig. 1, lanes 5–6), and polyclonal rabbit antiserum NW127 was generated against SDS gel-purified dynein HC (Fig. 1, lane 7).

*Dictyostelium* dynein IC is 39% identical and 56% similar to the rat IC, and 24% identical and 48% similar to the axonemal dynein IC sequence. In vitro binding studies have mapped the p150/Glued binding domain to the NH<sub>2</sub>-terminal 123 amino acids of rat dynein IC (Vaughan and Vallee, 1995). Although the primary sequences of *Dictyostelium* and rat dynein IC are very divergent (26% identical) at the NH<sub>2</sub> terminus, their predicted secondary struc-

tures are similar. Both have a coiled-coil domain near the NH<sub>2</sub> terminus followed by a serine-rich region. The structural similarity suggests that this region of the *Dictyostelium* IC is likely the dynactin binding domain. In contrast to the NH<sub>2</sub>-terminal domain, the COOH-terminal half of *Dictyostelium* and rat IC show 71% identity, suggesting that this domain may be involved in a conserved dynein IC function such as binding to other dynein subunits. Our hypothesis was that the NH<sub>2</sub>-terminal domain of IC is important for targeting dynein activity such as binding to dynactin, whereas the COOH terminus is crucial for dynein HC binding.

### Overexpression of Dynein IC Truncation Mutants

To functionally define the domains of dynein IC and to generate cell lines with defective dynein function, we overexpressed different IC domains in wild-type *Dictyostelium*. We designed several dynein IC truncation mutants that deleted or disrupted the hypothetical HC binding domain or the predicted dynactin binding domain (Fig. 2 A). IC $\Delta$ C lacks the COOH-terminal 373 amino acids, whereas IC $\Delta$ N47 and IC $\Delta$ N106 lack the NH<sub>2</sub>-terminal 47 or 106 residues, respectively. Mutant IC expression was controlled by a discoidin promoter, whose activity can be repressed by addition of folate to the medium (Blusch et al., 1992). This system makes it possible to conditionally express potentially deleterious mutants in *Dictyostelium*. Mutant protein expression was assessed using Western blots of whole cell lysates from cells induced for 3 d with IC-specific IC144 antibody (Fig. 2 B). For all three mutants, the mutant expression level was >10 times that of the endogenous wild-type IC.

### IC $\Delta$ C and IC $\Delta$ N Mutants Disrupted Dynein–Dynactin Interaction by Binding to One Complex but Not the Other

In vitro studies indicated that dynein IC can associate directly with dynactin complex and thus could serve as a link between the two large complexes (Karki and Holzbaur, 1995; Vaughan and Vallee, 1995). To test the IC truncation mutants for binding to either complex, we immunoprecipitated dynein with a dynein HC antibody (NW127) and dynactin using an affinity-purified capping protein  $\beta$  antibody (R18) (Hug et al., 1995; Schafer et al., 1994).

From wild-type *Dictyostelium* lysates, the endogenous IC coprecipitated with both NW127 and R18 antibody (Fig. 3), suggesting that wild-type IC associates with both dynein and dynactin complexes. However, each of the IC truncations was deficient in association with one of the two complexes. Although a significant amount of IC $\Delta$ C was detected in the capping protein IP, very little was detectable in dynein HC IP (Fig. 3). This suggests that the COOH-terminal deletion abolished the ability of IC to bind to dynein HC while preserving its dynactin binding activity. In contrast, both IC $\Delta$ N106 and IC $\Delta$ N47 mutants bound dynein HC well but associated poorly with dynactin. The ratio of IC $\Delta$ N to endogenous IC associated with dynactin is greatly reduced when compared with their ratio in cell lysates (Fig. 3). This suggests that the NH<sub>2</sub>-terminal IC region is crucial for dynactin association and is consistent with previous studies that mapped the p150

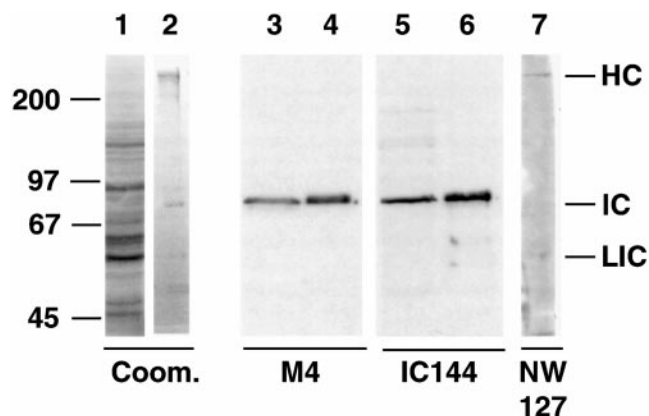


**Figure 1.** *Dictyostelium* dynein antibodies. *Dictyostelium* whole cell extracts (lanes 1, 3, and 5) and purified dynein (lanes 2, 4, 6, and 7) were separated on 7.5% SDS-polyacrylamide gels. Gel strips were stained with Coomassie blue (lanes 1 and 2) and Western blots probed with anti-IC antibodies M4 (lanes 3 and 4), IC144 (lanes 5 and 6), or with anti-HC antibody NW127 (lane 7). Positions of dynein subunits are indicated on the right; molecular mass markers (in kD) are indicated on the left. The 55-kD doublet in lane 2 is contaminating tubulin.

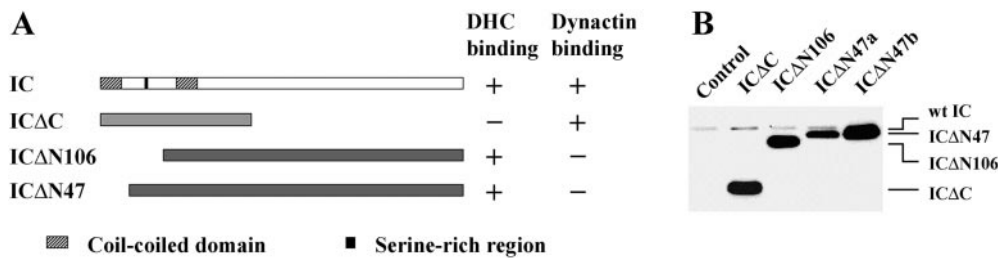


**Figure 2.** Structure and expression of dynein IC truncation mutants. (A) Diagram of predicted IC domain structure in relation to the IC truncations used in this study. ICΔC consists of amino acids 1-278 of the IC sequence. ICΔN106 deletes the NH<sub>2</sub>-terminal 106 amino acids, whereas ICΔN47 removes

the NH<sub>2</sub>-terminal 47 amino acids. (B) IC truncation mutants are expressed at high levels in wild-type *Dictyostelium*. Whole cell lysates ( $2 \times 10^5$  cells) were separated on a 7.5% SDS-PAGE gel and the blot probed with IC144 antibody. Control was wild-type cells transformed with pVEII vector alone. ICΔN47a and ICΔN47b are two independent cell lines that differ in their mutant protein expression level. The lower level of ICΔN47 expression in ICΔN74a allows visualization of both endogenous and mutant IC.

binding activity to the NH<sub>2</sub>-terminal region (Vaughan and Vallee, 1995). ICΔN47 showed better HC binding than ICΔN106, indicating that whereas the COOH-terminal conserved region of IC is required for dynein HC association, the binding is stabilized by residues that extend into the NH<sub>2</sub>-terminal domain.

To further investigate the dynein complex in IC mutant cells, cell lysates were fractionated on a 5-20% sucrose density gradient. Wild-type dynein migrated as a 20S complex containing both the HC and IC (Fig. 4). In ICΔC cells, ICΔC protein did not cosediment with the dynein HC and

wild-type IC (Fig. 4), providing independent evidence that this mutant failed to associate with dynein. Also, since wild-type IC comigrated with HC, dynein complex was not affected by ICΔC expression. For both ICΔN47 and ICΔN106 cells, a significant amount of the mutant IC cosedimented with HC at the normal position for dynein. The ratio of mutant IC to wild-type IC in the dynein fractions was consistent with that in dynein IPs, with the majority of dynein complexes containing the truncated IC mutant. In ICΔN106, a large amount of the mutant IC migrated near the top of the gradient, most likely due to its high expression level.

These results demonstrate that the IC truncation mutants are defective in their ability to mediate dynein-dynactin association, since they efficiently bind to only one partner but not the other. Therefore, overexpression of these truncated ICs would compete with endogenous wild-type IC for binding to one of the two partners, thereby disrupting the dynein-dynactin association. Consistent with this, there was less wild-type IC bound to HC in ICΔN-expressing cells, and greatly reduced wild-type IC in capping protein IPs in ICΔC expressing cells (Figs. 3 and 4).

### IC Mutants Exhibited Enlarged Morphology

We analyzed the three different IC mutant cell lines to determine the consequence of mutant IC expression. Interestingly, all three mutants produced similar phenotypes by affecting a range of dynein-dependent functions. By phase-contrast microscopy, induced mutant cells appeared larger and flatter than control or uninduced mutant cells (Fig. 5). To control for nonspecific effects due to high level exogenous protein expression, we also expressed full-length myc-tagged IC at levels similar to the mutants. None of the abnormalities seen in the mutants were observed (data not shown).

### IC Mutant Expression Resulted in Dispersed Localization of the Golgi Complex

Several studies have highlighted the importance of cytoplasmic dynein in Golgi apparatus positioning (Corthesy-Theulaz et al., 1992; Burkhardt et al., 1997; Harada et al., 1998). Therefore, Golgi complex localization is a good *in vivo* indicator of cytoplasmic dynein and dynactin function. Localization of the Golgi complex was detected by indirect immuno-

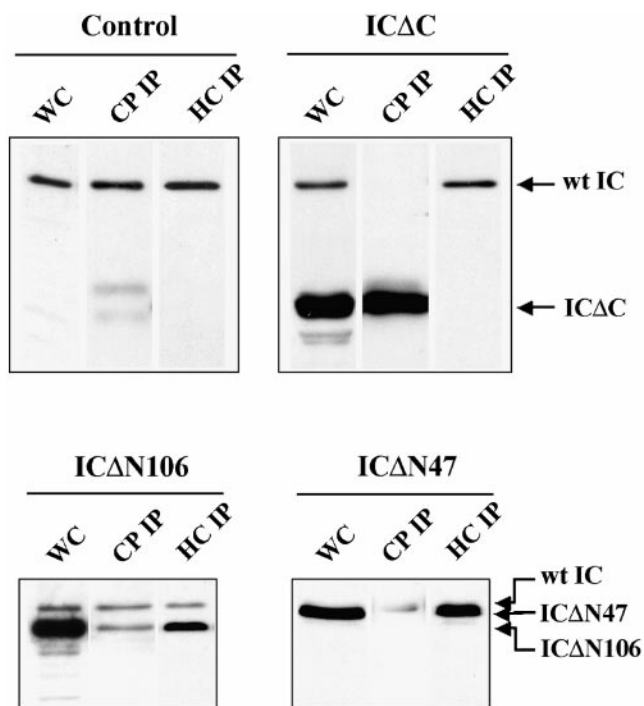


**Figure 3.** ICΔC binds dynactin but not dynein, whereas ICΔN associates with dynein but associates poorly with dynactin. Protein samples of cell lysates (WC) or immunoprecipitates (IP) from ICΔC cells, ICΔN cells, or vector controls were probed with IC144 antibody. Dynein was immunoprecipitated using the NW127 HC antibody (HC IP) and dynactin was immunoprecipitated using the capping protein  $\beta$  antibody R18 (CP IP). The faint double bands at the lower part of the CP IP lanes in control and ICΔC panels are Ig HCs.

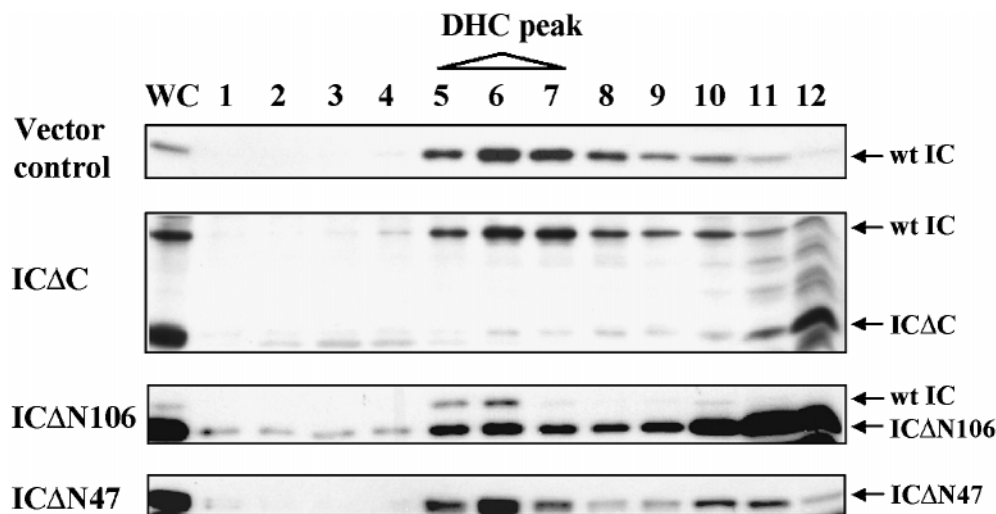


**Figure 4.** ICAN but not ICΔC cosediments with 20S dynein in sucrose gradients. Cell lysates were fractionated by centrifugation in 5–20% sucrose density gradient and equal volumes of the fractions separated by 7.5% SDS-PAGE. The positions of wild-type and mutant IC were detected with the IC144 antibody; IC mutants were also confirmed by 9E10 mAb that recognizes the myc tag (data not shown). Dynein HC, detected with NW127 antibody, sedimented in fractions 5–7. Cells analyzed are indicated on the left and the positions of relevant proteins are indicated on the right.

fluorescence using a mAb against comitin (Weiner et al., 1993). In wild-type *Dictyostelium* cells, the Golgi complex appears as a compact perinuclear cluster whose center coincides with the MT organizing center (MTOC) (Fig. 6 a). In contrast, in all three IC mutants the Golgi complex was dispersed throughout the cytoplasm (Fig. 6, c and e), supporting the idea that ICAN and ICΔC expression disrupted dynein function.

**IC Truncation Mutants Disrupted the Interphase MT Network and Led to Accumulation of Abnormal DNA Content**

Consistent with the change in cell morphology in the IC mutants, we observed dramatic changes in the organization of the MT network. Cells induced for 3 d were analyzed by indirect immunofluorescence with tubulin anti-

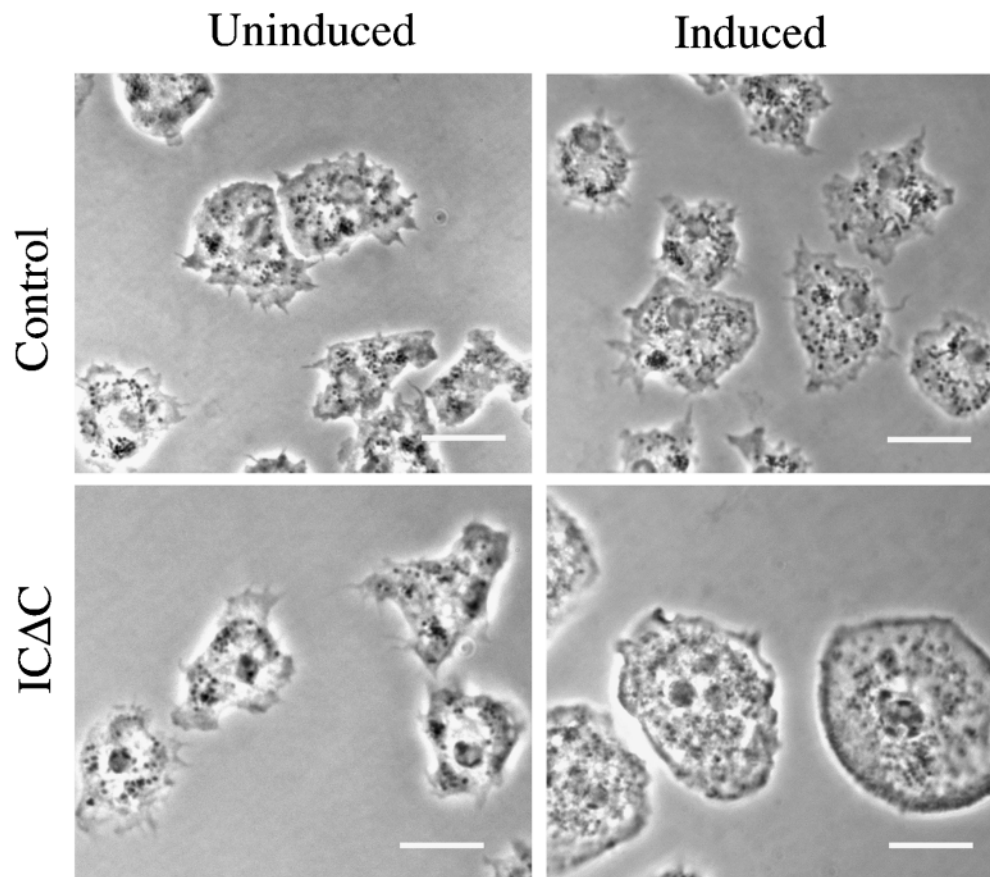


**Figure 5.** Cells expressing IC mutants are larger and flatter than wild-type cells. Phase contrast images of ICΔC or control cells cultured on coverslips for 3 d with or without induction are presented. Bars, 10 μm.

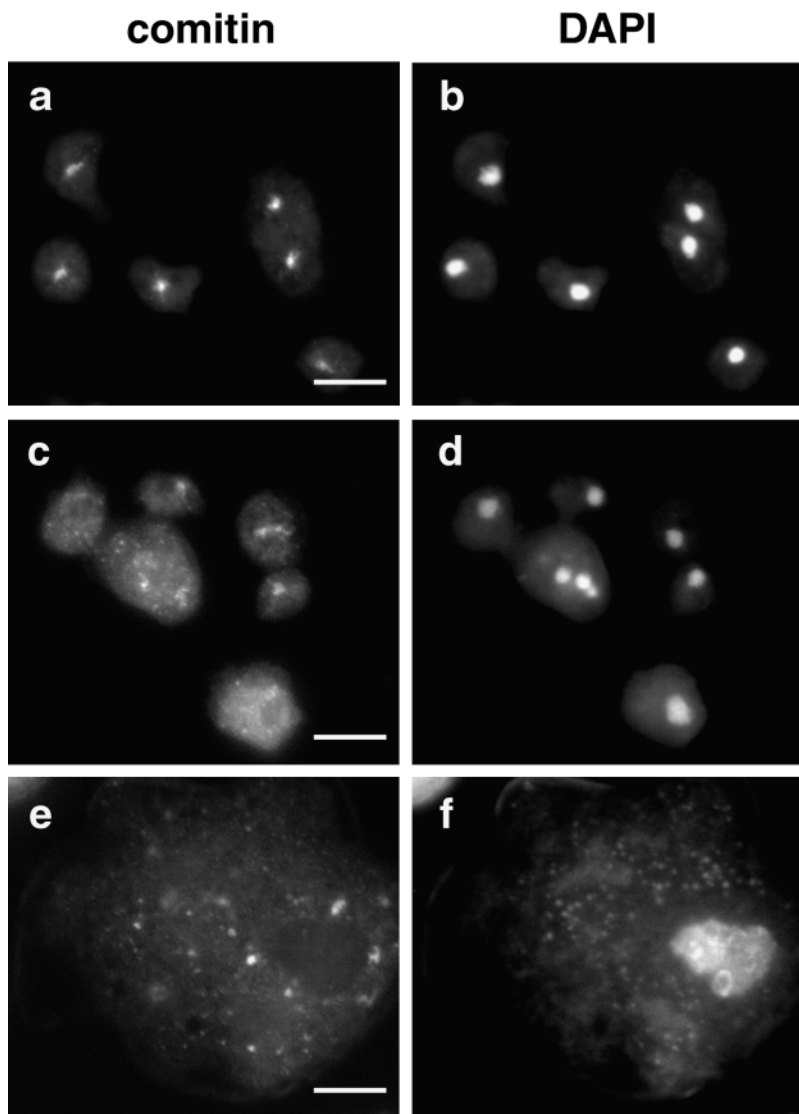


**Figure 6.** IC mutants cause Golgi dispersion. Control cells (a and b) or IC truncation mutant expressing cells (c–f) induced for 2 d were double-labeled with a comitin mAb to localize the Golgi complex (a, c, and e) and DAPI to visualize the nucleus (b, d, and f). All three IC truncations produced dispersion of the Golgi complex; IC $\Delta$ C shown (c and e). c and d show IC mutant cells with normal size, whereas e and f show IC mutants with the larger flattened morphology. Bars, 10  $\mu$ m.

body and DAPI staining of DNA. In wild-type cells (Fig. 7 a), interphase MTs formed extended radial arrays originating from the MTOC (Roos et al., 1984).

However, in both IC $\Delta$ C and IC $\Delta$ N cells, the interphase MTs were profoundly disorganized. The most striking phenotype was that the majority of the mutant cells showed the MT network collapsed into a bundle (Fig. 7 c). The MTOC of the bundles were often displaced to the cell periphery. Some cells showed a large yet relatively normal looking MT network (Fig. 7 e). The MTOC in both groups of cells were larger than normal, appearing as a large ring with a hollow center. As discussed below, the centrosomes in these cells were also abnormally large.

We also observed other MT abnormalities in a small number of mutant cells. Some cells exhibited multiple cytoplasmic MT asters (Fig. 7 g), some of which were nucleus-associated, whereas many were not. Occasionally we observed cells lacking obvious MT organization (Fig. 7 i), in which individual MTs were randomly distributed instead of focusing to an organizing center.

Mutant cells with MT abnormalities often showed big ir-

regular interphase nuclei with abnormal DNA distributions. We performed FACS<sup>®</sup> analysis to characterize the total DNA content in individual cells (Fig. 7 k). The vast majority of wild-type cells contained 2 N DNA, with a minor peak at 4 N (Fig. 7 k, dashed line). In contrast, the majority of IC $\Delta$ C cells contains >2 N DNA. Furthermore, the major peak of the mutant cells fell somewhere between 2 N and 4 N, and the rest had a wide range of DNA content that was not a multiple of the normal. This result suggests that the mutant cells were aneuploid, probably due to defects in chromosome segregation.

The abnormal nuclear DNA content and decreased viability (discussed below) of IC mutants suggested that the IC truncations caused defects in mitosis. Yet as judged by tubulin and DAPI staining, there was no increase in the mitotic index after induction. Like control cells, <2% of the induced IC mutant cells were in mitosis. Of the small numbers of mitotic spindles observed, some seemed normal, and others were monopolar or multipolar. In general, cells expressing IC truncations did not accumulate in mitosis, although there was clearly a mitotic defect.

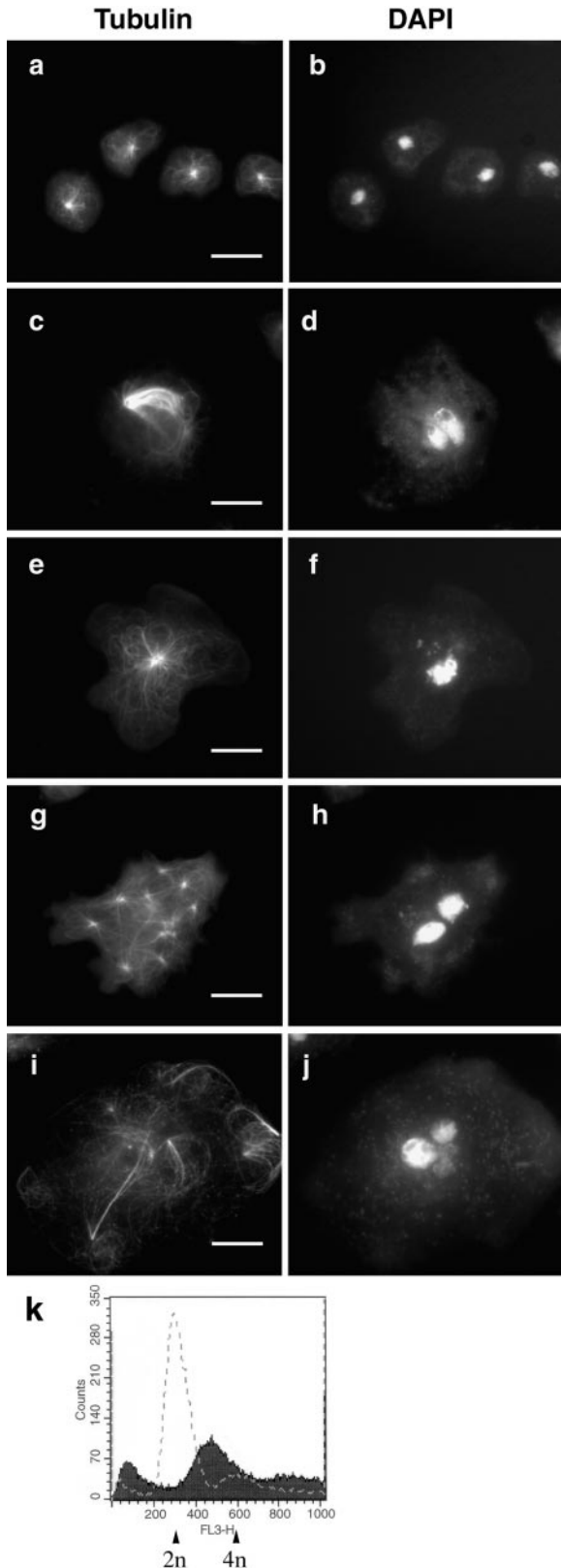


**Figure 7.** IC mutants alter MT networks, nuclear morphology, and DNA content. Vector controls (a and b) or cells expressing IC truncations (c–j) were stained with antitubulin mAb (a, c, e, g, and i) and DAPI (b, d, f, h, and j). ICΔC and ICΔN showed a similar range of phenotypes; ICΔC cells shown. d, f, h and j show altered nuclear morphology resulting from IC mutant expression.

### ***Dynein IC Mutant Expression Produced Centrosome Abnormalities***

Because of the profound MT disorganization, we next focused our attention on the MTOC or centrosome. We examined the centrosomes by indirect immunofluorescence using antibodies specific for several *Dictyostelium* centrosomal components (NAB350, 4/148, 2/165, and  $\gamma$ -tubulin) (Kalt and Schliwa, 1996; Euteneuer et al., 1998; Graf et al., 1998). All four antibodies have been shown to stain the corona of *Dictyostelium* centrosomes, which appear as dots by immunofluorescence. Over 99% of wild-type cells showed a single centrosome of uniform shape and size associated with the periphery of each nucleus (Fig. 8 a). However, all three IC truncation mutants showed a variety of centrosome abnormalities, including alterations in size, shape, number, and position. The centrosome abnormalities were rare in repressed cells, but dramatically increased upon induction.

The most frequent abnormality in the IC mutants was an enlarged centrosome associated with an enlarged nucleus (Fig. 8 c), or less frequently, with multiple nuclei (Fig. 8 e). Interestingly, the increased size and intensity of the centrosomes almost always correlated with increased cell size and nuclear DNA content. Occasionally elongated or dumbbell-shaped centrosomes were observed, which seemed to be two centrosomes closely adjacent to each other (Fig. 8 g), a pattern not observed in wild-type interphase cells. This strongly suggests that the abnormally large centrosomes may result from failed centrosome separation after duplication. We also observed a small number of IC mutant cells with multiple centrosomes and only one or two nuclei (Fig. 8 i), especially late in the induction course. Whereas some of these centrosomes were nucleus-associated, many were not.

To examine whether the centrosome and MT abnormalities were related, we double-labeled the centrosome and tubulin (Fig. 8, k and l). Except in cells with no apparent MT organization, centrosomal components always colocalized with the centers of MT asters. The abnormal size and number of centrosomes correlated with the abnormal size and number of MT networks.

### ***Time Course of MT and Centrosome Abnormalities***

To better understand the effect of IC mutations on MT organization and centrosome morphology, we determined MT and centrosome morphology at various timepoints after induction (Fig. 9). The phenotypes fell into one of five categories: (1) normal MT network; (2) bundled MTs; (3) large centrosomes; (4) multiple MT asters; and (5) disorganized MT without an obvious organizing center. Before induction (day 0), >90% of the ICΔC cells had normal MT

Mutant morphologies include collapsed MT networks forming bundles (c), unusually large MT network with large MTOC (e), multiple cytoplasmic asters (g), and poorly organized MTs lacking a visible organizing center (i). Bars, 10  $\mu$ m. k shows a typical FACS<sup>®</sup> profile of control or ICΔC cells induced for 2 d. The x-axis shows the DNA content and y-axis shows the cell count. The dashed line represents controls and the shaded area represents ICΔC cells. 50,000 cells were analyzed for each sample.

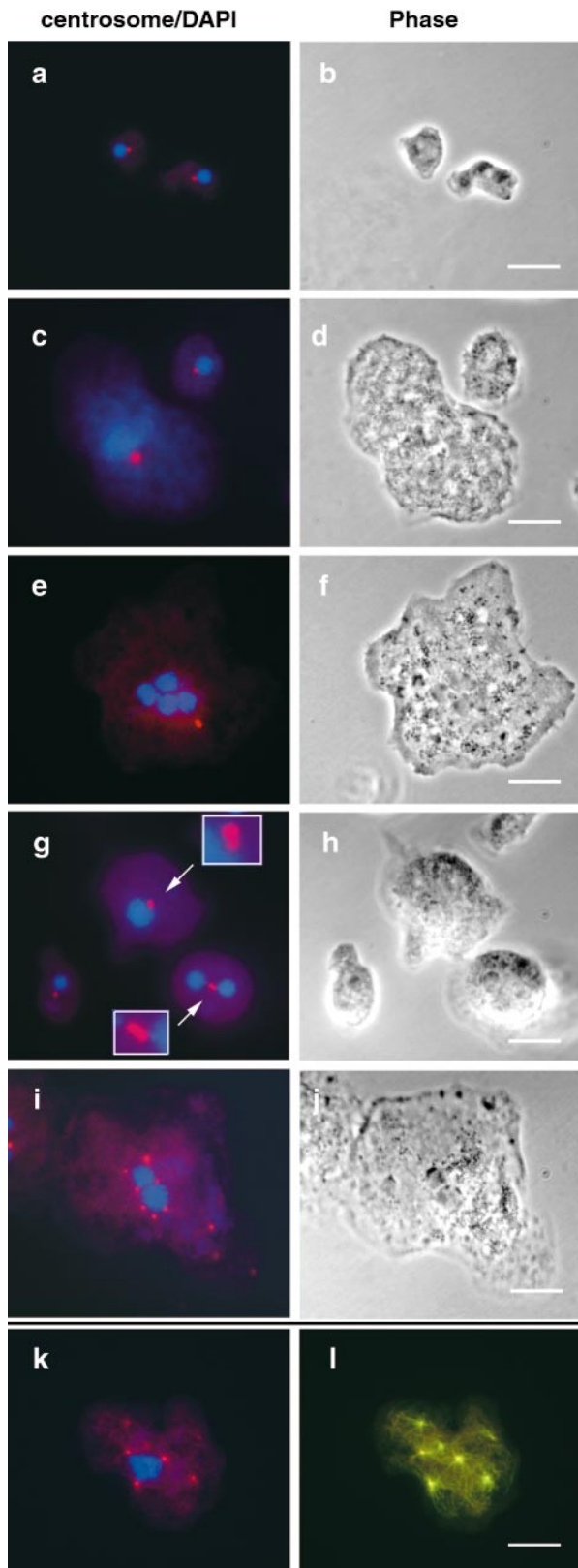


**Figure 8.** Expression of IC truncations produces centrosome abnormalities. Vector control cells (a and b) or cells expressing IC truncations (c–l) were labeled with centrosome antibodies (red), and DAPI (blue) (a, c, e, g, i, and k). l shows an overlay of centrosome (red) and tubulin (green) staining, with the overlapping area in yellow. b, d, f, h and j show phase-contrast images. Cen-

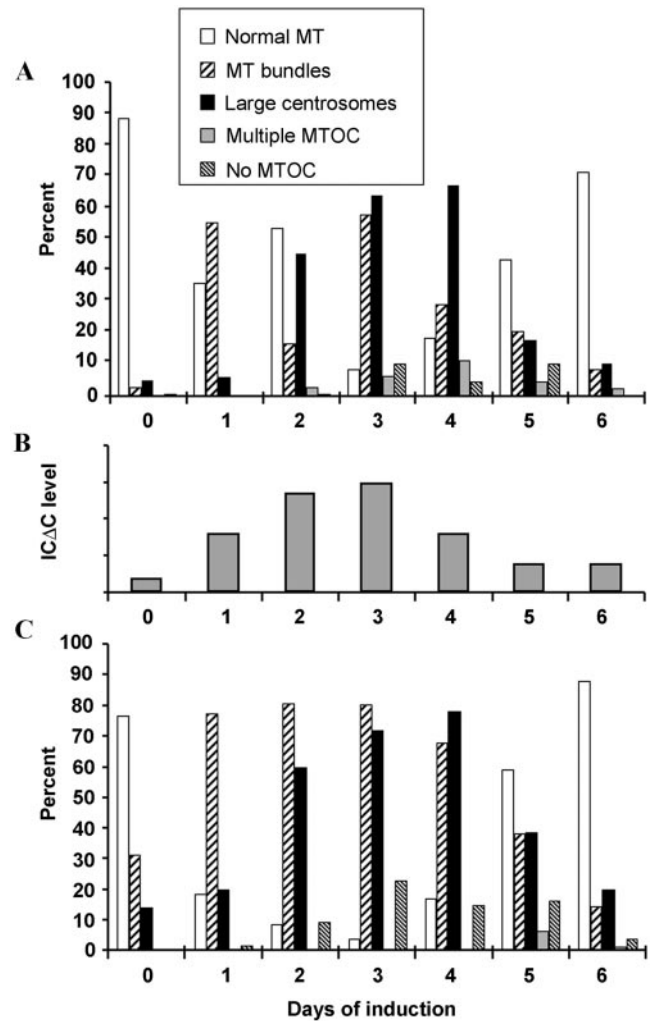


**Figure 9.** Time course of MT and centrosome phenotypes. Mutant cells grown under repressed conditions were induced. Samples taken daily were fixed and stained with tubulin and centrosome-specific antibodies. The percentage of ICΔC cells (A) and ICΔN47 cells (C) showing normal MT organization, MT bundling, large centrosomes, multiple MT asters, or MTs without an organizing center on each day are presented. B shows the level of ICΔC mutant protein expression determined by densitometric analysis on Western blots of cell lysates.

networks and centrosomes (Fig. 9 A). 1 d after induction, the MT network was bundled in >50% of the cells, although the sizes of the centrosomes were normal. As induction proceeded, the cells, their MT networks, and their centrosomes became enlarged. On day 3 after induction, ~60% of the cells had large MT bundles and ~70% showed large centrosomes. The large MT networks were usually accompanied by large centrosomes and large nu-

clei (c) or with multiple nuclei (e); dumbbell-shaped centrosomes (g); and multiple centrosomes (i and k). In cells with multiple centrosomes each centrosome organizes MTs (l). Bars, 10  $\mu$ m.



clei. Less than 10% of the cells showed relatively normal MT networks. However after 4 d, the number of cells with normal MT networks began to increase. By day 6, 73% of the population had normal MTs and centrosomes.

This time course established two primary phenotypes: MT bundling and unusually large centrosomes. MT bundling became apparent very early after induction and peaked by 3 d. The large centrosomes appeared on day 2 and peaked on day 3. Whereas disruption of the MT network occurred once the level of mutant IC became high enough to disrupt dynein function, the effect on centrosomes occurred only after mitosis. Peak expression of the phenotypic defects correlates with the level of mutant IC (Fig. 9 B). Accordingly, after day 4, ICΔC expression decreased, leading to increased number of cells with normal MT networks.

A similar pattern was observed in ICΔN47 cells (Fig. 9 C). MT bundling and large centrosomes appeared and peaked around the same time as in ICΔC cells. ICΔC and ICΔN mutants had similar effects on dynein function, further suggesting that the major function of the IC is to mediate dynein–dynactin interaction, and that most dynein functions require dynactin association.

The return of normal MT organization along with decreasing mutant expression could occur because the mutant phenotype was reversible, or because the severely affected cells died and were eventually outgrown by cells that no longer expressed the IC truncation. Therefore, we determined cell viability after induction by measuring the plating efficiency. In contrast to 91% for wild-type, ICΔC cells induced for 3 d had a plating efficiency of 12%, indicating that mutant cells had significantly decreased viability. The number of viable mutant cells was comparable to the number with normal MT networks (9%), consistent with the idea that cells with MT or centrosome abnormalities may be nonviable, most likely due to mitotic defects.

### IC Mutations Affected Centrosome Replication and Separation

One striking phenotype of IC mutants was the presence of apparently larger centrosomes. Apparently large centrosomes in the light microscope could result from closely positioned, morphologically normal centrosomes produced by defective centrosome duplication or separation, or from the abnormal accumulation of centrosomal material. To distinguish these possibilities, we examined centrosome morphology at the ultrastructural level. The interphase *Dictyostelium* centrosome is a nucleus-associated body consisting of a rectangular, electron-dense core surrounded by an amorphous matrix or corona from which MTs radiate (Fig. 10 a) (Moens, 1976; Kuriyama et al., 1982; Omura and Fukui, 1985). The core is a tripartite structure of  $\sim 280 \times 220 \times 130$  nm in size (Ueda et al., 1999). As expected, the length of wild-type centrosome cores averaged  $285 \pm 45$  nm, whereas the ICΔC mutants were substantially larger, averaging  $387 \pm 104$  nm in length, with some nearly twice the length of wild-type (Fig. 10, b–d). The tripartite organization of the core and the corona of these long centrosomes appeared similar to wild-type. The observation of centrosomes twice the normal length in interphase cells suggests they may arise from failure of the centrosome replication cycle which normally doubles the length of centrosomes during prophase and then separates the two halves longitudinally to produce the spindle poles (Ueda et al., 1999).

We also observed paired centrosomes in interphase ICΔC cells (Fig. 10, e–h). In these pairs, two centrosomes were  $<300$  nm apart, a configuration not seen in wild-type cells. The large centrosomes detected by fluorescence microscopy represented both longer and closely paired centrosomes. These abnormalities suggest that dynein mutants are defective in centrosome replication or separation.

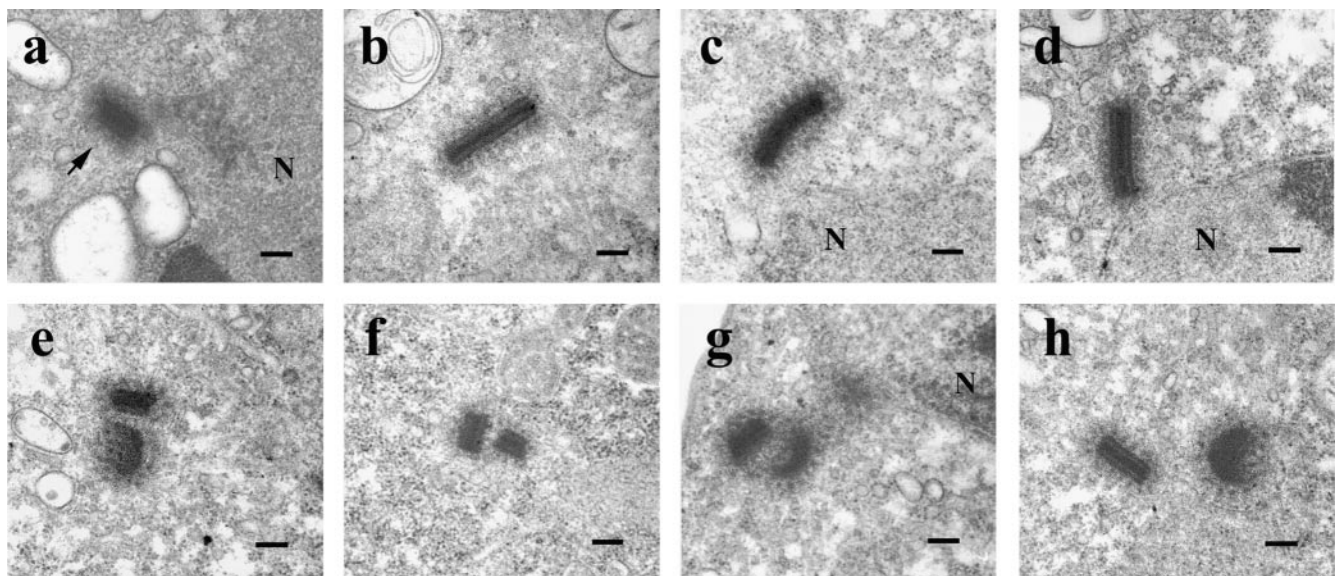


**Figure 10.** IC truncations produced centrosomes with increased core lengths and failure to separate. Wild-type (a) or ICΔC cells (b–h) induced for 2 d were analyzed for centrosome morphology by EM. All cells shown are in interphase. A wild-type centrosome (a) is indicated by the arrowhead. (b–d) ICΔC cells with centrosome cores longer than wild-type. (e–h) ICΔC cells showing paired centrosomes suggesting separation defects. N, nucleus. Bars, 200 nm.

## Discussion

In this study we tested the hypothesis that IC-mediated dynein–dynactin interaction is required for dynein-dependent functions *in vivo* by expressing IC truncation mutants in wild-type *Dictyostelium* cells. The NH<sub>2</sub>-terminal domain bound only dynactin, whereas the COOH-terminal domain associated with dynein. When overexpressed, both NH<sub>2</sub>-terminal and COOH-terminal mutants resulted in dispersion of the Golgi complex, as expected for defective dynein function (Corthesy-Theulaz et al., 1992; Burkhardt et al., 1997; Harada et al., 1998). We also found a variety of additional phenotypes, including dramatic alteration in the MT network, changes in centrosome size and number, and altered nuclear DNA content. These results demonstrate the essential role of the IC in mediating dynein–dynactin interaction *in vivo*, and suggest that this interaction is important for most dynein-dependent cellular functions. In addition, this study revealed a novel role for dynein in centrosome replication and separation.

### Association of the IC with Dynein

The ability of ICΔN47 and ICΔN106 to associate with dynein, together with ICΔC's failure to bind, shows that the COOH-terminal domain of the IC is required for HC association. ICΔN47 bound the HC more efficiently than did ICΔN106, whereas a more extended NH<sub>2</sub>-terminal truncation, ICΔN278, associated only weakly with the HC (data not shown). The IC is a WD-repeat-containing protein (Wilkerson et al., 1995). Analysis of the *Dictyostelium* IC predicts presence of six WD domains located in the COOH-terminal half of the molecule. Since ICΔC, with the WD-repeats deleted, was unable to bind to HC, WD domains seem to be required for HC association. However, even the largest NH<sub>2</sub>-terminal truncation, ICΔN278, which has intact WD repeats, failed to efficiently bind the HC, suggesting that the WD repeats are not sufficient for HC binding. The prediction of six potential β-propeller structures suggests that the IC adopts a structure similar to the G protein β subunit (Neer et al., 1994; Lambright et al., 1996). In this model the loops that connect the β-propellers on one face of the IC would bind the HC, leaving the loops on the opposite side of the propeller available for another association. However, as is the case for Gβ association with Gγ, an extended region (residues 107–278) containing a predicted coiled-coil domain appears important for stable IC–HC association.

### IC Mediates Dynein–Dynactin Interaction *In Vivo*

The IC could contribute to dynein function by: (a) facilitating dynein–dynactin interaction, thus targeting dynein to specific cargos via dynactin; (b) regulating dynein enzymatic activity; or (c) mediating the association of other subunits with the dynein complex. *In vitro* studies showed that IC interacts with p150 subunit of dynactin, providing a link between dynein and dynactin (Karki and Holzbaaur, 1995; Vaughan and Vallee, 1995). Our results provide direct evidence for dynein–dynactin interaction *in vivo* by showing that the IC associated with both complexes in immunoprecipitates of the cell lysates. In ICΔN cells, most dynein molecules carry truncated IC subunits defective in

dynactin binding. In contrast, in ICΔC cells, the dynein complex was intact and only its association with dynactin was blocked. Since the ICΔN and ICΔC mutants produced indistinguishable phenotypes (Fig. 9, A and C), it is likely that a primary role of the IC is to mediate dynein–dynactin interaction. However, this does not exclude the possibility that the IC may regulate dynein by additional means.

### Cytoplasmic Dynein Is Essential for *Dictyostelium*

As a first approach to study IC function, we attempted to generate *Dictyostelium* cell lines with a disrupted IC gene but never obtained IC-null mutants. Combined with the failure to generate dynein HC-null lines in *Dictyostelium* (Koonce and Knecht, 1998), this strongly suggests that dynein function is required for the viability of *Dictyostelium* cells. Therefore, we expressed IC truncation mutants controlled by an inducible promoter to disrupt dynein function in a regulated fashion. When repressed, cells carrying the mutant expression construct grew well. However, upon induction, viability decreased as abnormal phenotypes appeared. Judged by plaque formation on bacterial lawns, only 12% of the cells were viable 3 d after induction, further confirming that dynein function is essential for *Dictyostelium* viability. Previous studies on cytoplasmic dynein have revealed different requirements for dynein in other organisms. Dynein function is not essential for yeast and filamentous fungi, including *Neurospora* and *Aspergillus*, whereas dynein is required for the viability of *Drosophila* and mammalian cells (Eshel et al., 1993; Vaisberg et al., 1993; Plamann et al., 1994; Xiang et al., 1994; Echeverri et al., 1996; Gepner et al., 1996). In this regard, *Dictyostelium's* dynein requirement is similar to that of higher eukaryotic systems.

How does dynein affect cell viability? The centrosome and nuclear abnormalities in the IC mutants indicate mitotic defects. Large centrosomes likely result from failure of centrosome separation after its duplication in prophase. Subsequent failure of spindle formation or separation would affect chromosome separation producing the aneuploidy we observed. This idea is supported by the observation of large centrosomes and increased nuclear DNA content only when induction exceeded one cell cycle.

Cells unable to accomplish mitosis might be expected to arrest in mitosis due to a mitotic checkpoint mechanism. However, we did not see an increase in mitotic index in IC mutants. Cells with large centrosomes and abnormal nuclei appeared to be in interphase. This suggests that *Dictyostelium* cells can bypass the mitotic checkpoint. Consistent with this, *Dictyostelium* cells treated with MT-disrupting drugs such as nocodazole showed only a transient increase in mitotic index that then returned to normal (Welker and Williams, 1980). However such cells were inviable, consistent with the decreased viability we observed.

### Dynein Function Is Required for Organizing the Interphase MT Network

Expression of IC truncation mutants in wild-type *Dictyostelium* cells resulted in dramatic changes in the interphase MT network. The most dominant phenotype was the collapse of normally radial MT arrays into bundles. This indi-

cates a role for dynein–dynactin interaction in the organization of interphase MTs. The transition of well-extended radial MT arrays to bundles when dynein function was disrupted suggests a change in the balance of the forces responsible for the normal extended morphology of the MT network.

A similar MT bundling phenotype has been observed in *Dictyostelium* cells overexpressing the head domain of the HC (Koonce and Samsó, 1996). Based on this, dynein was proposed to provide a traction force to keep the MTs extended as a radial array (Koonce, 1996; Koonce and Samsó, 1996). Our results support this model. As a minus end–directed MT-based motor, dynein has the proper polarity to generate a traction force on the MTs, provided it has an anchoring point. Dynein and dynactin have been localized on both membranous organelles and the cell cortex (Bomsel et al., 1990; Lin and Collins, 1992; Yu et al., 1992; Vallee and Sheetz, 1996; Hirokawa, 1998; Skop and White, 1998). Dynein–dynactin anchored at the cell cortex could provide a point of attachment acting as a tension generating element that holds the plus-ends of MTs in place. Similarly, dynein–dynactin anchored on cellular organelles such as the nucleus and vesicles could also provide a traction force along the sides of MTs. Release of this connection by disrupting the dynein–dynactin interaction could collapse the MT network.

### ***Dynein Is Required for Centrosome Replication and Separation***

Perhaps the most striking phenotype of the IC truncation mutants was the abnormal centrosome morphology, suggesting defects in centrosome replication and separation. Centrosomes duplicate once each cell cycle. Daughter centrosomes separate early in mitosis to form the spindle poles, and after mitosis, become the MTOCs for the daughter cells. In *Dictyostelium*, the interphase centrosome has a box-shaped, multilayered core. In prophase the three-layered core doubles in length and then splits longitudinally to expose an inner face that nucleates polar and kinetochore MTs in prometaphase. The spindle then elongates to separate the chromosomes in anaphase, and finally, at the end of telophase, the mitotic centrosomes fold in half to reform the interphase length, three layered centrosome (Ueda et al., 1999).

The large centrosomes in the IC mutant cells appear to result from failure of the centrosome replication cycle. The elongated centrosomes observed during interphase have the morphology of prophase centrosomes, suggesting that the lengthwise separation of prophase centrosomes requires dynein function. The failed replication would prevent the centrosome from effectively serving as spindle poles as they could not nucleate polar or kinetochore MTs. The resulting failure of chromosome separation would result in accumulation of abnormal DNA content, one of the phenotypes we observed.

Immediately after the longitudinal separation described above, the two mitotic centrosomes (now spindle poles) must separate in order to segregate chromosomes. The centrosome pairs we observed may be the result of failed spindle pole separation and/or elongation. This failure to separate, followed by the normal postmitotic folding,

would produce paired centrosomes. Failure of this step in the centrosome duplication would also lead to accumulation of abnormal DNA content seen in IC mutants.

Both centrosome phenotypes appear to result from a disrupted centrosome replication cycle caused by the expression of IC truncations. These results strongly suggest that dynein is required for the early steps in the centrosome replication, mitotic spindle formation, and/or elongation. This is consistent with the report that injection of function-blocking dynein HC antibody blocked spindle formation in cultured mammalian cells (Vaisberg et al., 1993).

How might dynein be involved in centrosome separation? One possible model is that dynein attached to some cellular anchor point, such as membranous organelles or the cell cortex, produces a minus end–directed force on the astral MTs that draws the two mitotic centrosomes apart. Alternatively, dynein could be required to transport a plus end–directed motor to the centrosome, and this plus end–directed motor actually provides the force for centrosome separation. Several kinesin-like proteins have been implicated in spindle pole separation (Barton and Goldstein, 1996; Walczak et al., 1998). Xklp-2, a plus end–directed kinesin-like protein is required for centrosome separation and the maintenance of bipolar spindles in *Xenopus* oocyte mitotic extracts. This function is dependent

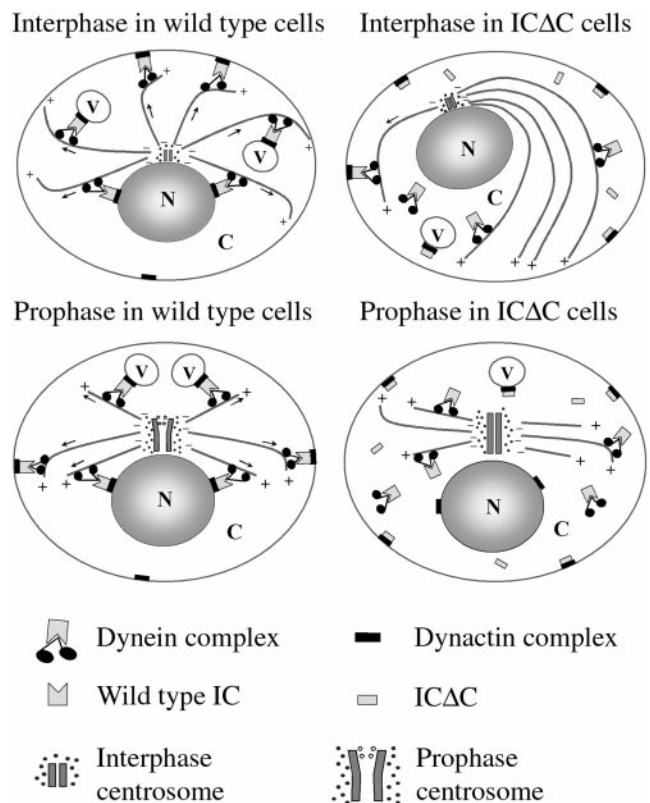


**Figure 11.** Model for the role of dynein in interphase MT organization and mitotic centrosome separation. Also shown is the mechanism by which IC truncation mutants might disrupt dynein function. N, nucleus; C, cytoplasm; V, membranous vesicles. Arrows indicate the direction of force applied on MTs by dynein. +/- depicts the ends of MTs. See Discussion for details.

on its proper localization to the spindle poles, which requires cytoplasmic dynein and dynactin function (Boleti et al., 1996; Wittmann et al., 1998). Therefore, defective dynein function may indirectly affect centrosome separation by affecting the localization of kinesin-like motors. Finally, it is possible that dynein exerts its effect indirectly by altering MT organization or dynamics.

### **Model for the Role of Dynein Function in MT Organization and Centrosome Separation**

In sum, our results, together with the work of others, suggests the model shown in Fig. 11 for the role of dynein in MT organization and centrosome separation. Dynein, acting through an association with dynactin, could produce traction forces acting either along the sides or on the plus-ends of cytoplasmic MTs to maintain the radial array or direct the movement of the MT network in interphase. During mitosis, the pulling force on astral MTs could facilitate centrosome replication and spindle pole separation. Cytoplasmic dynein might exert such plus-end-directed forces on MTs and centrosomes by anchoring on membranous organelles, including the nuclear membrane or cell cortex. This anchoring of cytoplasmic dynein is dependent on its proper association with dynactin. The IC serves as a bridge between cytoplasmic dynein and dynactin complex and is crucial for their interaction. Overexpression of IC truncation mutants disrupts the binding of cytoplasmic dynein to dynactin, leading to dissociation of dynein from its cytoplasmic anchoring points. Without anchoring points, dynein could no longer produce tension on MTs, resulting in collapsed MT arrays and abolished centrosome separation.

We would like to thank Dr. John Cooper for providing the capping protein antibodies, and Dr. Angelika A. Noegel for providing hybridoma cell lines producing comitin monoclonal antibody. We thank Dr. Michael P. Koonce for inspiring discussion. We thank Maya Moody for assistance with the electron microscopy, and the members in the Chisholm lab for helpful discussions. Special thanks to Petra Fey for help in editing the manuscript.

This work was supported by a research grant from the National Institutes of Health to R.L. Chisholm (GM39264).

Submitted: 28 May 1999

Revised: 5 November 1999

Accepted: 5 November 1999

### **References**

Barton, N.R., and L.S. Goldstein. 1996. Going mobile: microtubule motors and chromosome segregation. *Proc. Natl. Acad. Sci. USA*. 93:1735-1742.

Blusch, J., P. Morandini, and W. Nellen. 1992. Transcriptional regulation by folate: inducible gene expression in *Dictyostelium* transformants during growth and early development. *Nucleic Acids Res.* 20:6235-6238.

Boleti, H., E. Karsenti, and I. Vernos. 1996. Xklp2, a novel *Xenopus* centrosomal kinesin-like protein required for centrosome separation during mitosis. *Cell*. 84:49-59.

Bomsel, M., R. Parton, S.A. Kuznetsov, T.A. Schroer, and J. Gruenberg. 1990. Microtubule- and motor-dependent fusion in vitro between apical and basolateral endocytic vesicles from MDCK cells. *Cell*. 62:719-731.

Bruno, K.S., J.H. Tinsley, P.F. Minke, and M. Plamann. 1996. Genetic interactions among cytoplasmic dynein, dynactin, and nuclear distribution mutants of *Neurospora crassa*. *Proc. Natl. Acad. Sci. USA*. 93:4775-4780.

Burkhardt, J.K., C.J. Echeverri, T. Nilsson, and R.B. Vallee. 1997. Overexpression of the dynamitin (p50) subunit of the dynactin complex disrupts dynein-dependent maintenance of membrane organelle distribution. *J. Cell Biol.* 139:469-484.

Clark, S.W., and D.I. Meyer. 1994. ACT3: a putative centractin homologue in *S. cerevisiae* is required for proper orientation of the mitotic spindle. *J. Cell Biol.* 127:129-138.

Corthesy-Theulaz, I., A. Pauloin, and S.R. Pfeffer. 1992. Cytoplasmic dynein participates in the centrosomal localization of the Golgi complex. *J. Cell Biol.* 118:1333-1345.

Dillman, J.F., III, L.P. Dabney, S. Karki, B.M. Paschal, E.L. Holzbaur, and K.K. Pfister. 1996. Functional analysis of dynactin and cytoplasmic dynein in slow axonal transport. *J. Neurosci.* 16:6742-6752.

Echeverri, C.J., B.M. Paschal, K.T. Vaughan, and R.B. Vallee. 1996. Molecular characterization of the 50-kD subunit of dynactin reveals function for the complex in chromosome alignment and spindle organization during mitosis. *J. Cell Biol.* 132:617-633.

Eshel, D., L.A. Urrestarazu, S. Vissers, J.C. Jauniaux, J.C. van Vliet-Reedijk, R.J. Planta, and I.R. Gibbons. 1993. Cytoplasmic dynein is required for normal nuclear segregation in yeast. *Proc. Natl. Acad. Sci. USA*. 90:11172-11176.

Euteneuer, U., R. Graf, E. Kube-Granderath, and M. Schliwa. 1998. *Dictyostelium* gamma-tubulin: molecular characterization and ultrastructural localization. *J. Cell Sci.* 111:405-412.

Gepner, J., M. Li, S. Ludmann, C. Kortas, K. Boylan, S.J. Iyadurai, M. McGrail, and T.S. Hays. 1996. Cytoplasmic dynein function is essential in *Drosophila melanogaster*. *Genetics*. 142:865-878.

Gill, S.R., T.A. Schroer, I. Szilak, E.R. Steuer, M.P. Sheetz, and D.W. Cleveland. 1991. Dynactin, a conserved, ubiquitously expressed component of an activator of vesicle motility mediated by cytoplasmic dynein. *J. Cell Biol.* 115:1639-1650.

Graf, R., U. Euteneuer, M. Ueda, and M. Schliwa. 1998. Isolation of nucleation-competent centrosomes from *Dictyostelium discoideum*. *Eur. J. Cell Biol.* 76:167-175.

Graf, R., C. Daunderer, and M. Schliwa. 1999. Cell cycle-dependent localization of monoclonal antibodies raised against isolated *Dictyostelium* centrosomes. *Biol. Cell*. 91:471-477.

Harada, A., Y. Takei, Y. Kanai, Y. Tanaka, S. Nonaka, and N. Hirokawa. 1998. Golgi vesiculation and lysosome dispersion in cells lacking cytoplasmic dynein. *J. Cell Biol.* 141:51-59.

Hirokawa, N. 1998. Kinesin and dynein superfamily proteins and the mechanism of organelle transport. *Science*. 279:519-526.

Howard, P.K., K.G. Ahern, and R.A. Firtel. 1988. Establishment of a transient expression system for *Dictyostelium discoideum*. *Nucleic Acids Res.* 16:2613-2623.

Hug, C., P.Y. Jay, I. Reddy, J.G. McNally, P.C. Bridgman, E.L. Elson, and J.A. Cooper. 1995. Capping protein levels influence actin assembly and cell motility in *Dictyostelium*. *Cell*. 81:591-600.

Kalt, A., and M. Schliwa. 1996. A novel structural component of the *Dictyostelium* centrosome. *J. Cell Sci.* 109:3103-3112.

Karki, S., and E.L. Holzbaur. 1995. Affinity chromatography demonstrates a direct binding between cytoplasmic dynein and the dynactin complex. *J. Biol. Chem.* 270:28806-28811.

Koonce, M.P. 1996. Making a connection: the "other" microtubule end. *Cell Motil. Cytoskelet.* 35:85-93.

Koonce, M.P., and J.R. McIntosh. 1990. Identification and immunolocalization of cytoplasmic dynein in *Dictyostelium*. *Cell Motil. Cytoskelet.* 15:51-62.

Koonce, M.P., and M. Samsó. 1996. Overexpression of cytoplasmic dynein's globular head causes a collapse of the interphase microtubule network in *Dictyostelium*. *Mol. Biol. Cell*. 7:935-948.

Koonce, M.P., and D.A. Knecht. 1998. Cytoplasmic dynein heavy chain is an essential gene product in *Dictyostelium*. *Cell Motil. Cytoskelet.* 39:63-72.

Kuriyama, R., C. Sato, Y. Fukui, and S. Nishibayashi. 1982. In vitro nucleation of microtubules from microtubule-organizing center prepared from cellular slime mold. *Cell Motil.* 2:257-272.

Lambright, D.G., J. Sondek, A. Böhm, N.P. Skiba, H.E. Hamm, and P.B. Sigler. 1996. The 2.0 Å crystal structure of a heterotrimeric G protein. *Nature*. 379:311-319.

Lin, S.X., and C.A. Collins. 1992. Immunolocalization of cytoplasmic dynein to lysosomes in cultured cells. *J. Cell Sci.* 101:125-137.

McGrail, M., J. Gepner, A. Silvanovich, S. Ludmann, M. Serr, and T.S. Hays. 1995. Regulation of cytoplasmic dynein function in vivo by the *Drosophila* Glued complex. *J. Cell Biol.* 131:411-425.

Moens, P.B. 1976. Spindle and kinetochore morphology of *Dictyostelium discoideum*. *J. Cell Biol.* 68:113-122.

Muhua, L., T.S. Karpova, and J.A. Cooper. 1994. A yeast actin-related protein homologous to that in vertebrate dynactin complex is important for spindle orientation and nuclear migration. *Cell*. 78:669-679.

Neer, E.J., C.J. Schmidt, R. Nambudripad, and T.F. Smith. 1994. The ancient regulatory-protein family of WD-repeat proteins [published erratum appears in *Nature* 371:812]. *Nature*. 371:297-300.

Omura, F., and Y. Fukui. 1985. *Dictyostelium* MTOC: structure and linkage to the nucleus. *Protoplasma*. 127:212-221.

Paschal, B.M., A. Mikami, K.K. Pfister, and R.B. Vallee. 1992. Homology of the 74-kD cytoplasmic dynein subunit with a flagellar dynein polypeptide suggests an intracellular targeting function. *J. Cell Biol.* 118:1133-1143.

Plamann, M., P.F. Minke, J.H. Tinsley, and K.S. Bruno. 1994. Cytoplasmic dynein and actin-related protein Arp1 are required for normal nuclear distribution in filamentous fungi. *J. Cell Biol.* 127:139-149.

Presley, J.F., N.B. Cole, T.A. Schroer, K. Hirschberg, K.J. Zaal, and J. Lippincott-Schwartz. 1997. ER-to-Golgi transport visualized in living cells. *Nature*. 389:81-85.

- Roos, U.P., M. De Brabander, and J. De Mey. 1984. Indirect immunofluorescence of microtubules in *Dictyostelium discoideum*. A study with polyclonal and monoclonal antibodies to tubulins. *Exp. Cell Res.* 151:183–193.
- Schafer, D.A., S.R. Gill, J.A. Cooper, J.E. Heuser, and T.A. Schroer. 1994. Ultrastructural analysis of the dynactin complex: an actin-related protein is a component of a filament that resembles F-actin. *J. Cell Biol.* 126:403–412.
- Schroer, T.A., and M.P. Sheetz. 1991. Two activators of microtubule-based vesicle transport. *J. Cell Biol.* 115:1309–1318.
- Skop, A.R., and J.G. White. 1998. The dynactin complex is required for cleavage plane specification in early *Caenorhabditis elegans* embryos. *Curr. Biol.* 8:1110–1116.
- Steffen, W., J.L. Hodgkinson, and G. Wiche. 1996. Immunogold localization of the intermediate chain within the protein complex of cytoplasmic dynein. *J. Struct. Biol.* 117:227–235.
- Tinsley, J.H., P.F. Minke, K.S. Bruno, and M. Plamann. 1996. p150Glued, the largest subunit of the dynactin complex, is nonessential in *Neurospora* but required for nuclear distribution. *Mol. Biol. Cell.* 7:731–742.
- Ueda, M., M. Schliwa, and U. Euteneuer. 1999. Unusual centrosome cycle in *Dictyostelium*: correlation of dynamic behavior and structural changes. *Mol. Biol. Cell.* 10:151–160.
- Vaisberg, E.A., M.P. Koonce, and J.R. McIntosh. 1993. Cytoplasmic dynein plays a role in mammalian mitotic spindle formation. *J. Cell Biol.* 123:849–858.
- Vallee, R.B., and M.P. Sheetz. 1996. Targeting of motor proteins. *Science.* 271:1539–1544.
- Vaughan, K.T., and R.B. Vallee. 1995. Cytoplasmic dynein binds dynactin through a direct interaction between the intermediate chains and p150-Glued. *J. Cell Biol.* 131:1507–1516.
- Walczak, C.E., I. Vernos, T.J. Mitchison, E. Karsenti, and R. Heald. 1998. A model for the proposed roles of different microtubule-based motor proteins in establishing spindle bipolarity. *Curr. Biol.* 8:903–913.
- Waterman-Storer, C.M., S.B. Karki, S.A. Kuznetsov, J.S. Tabb, D.G. Weiss, G.M. Langford, and E.L. Holzbaur. 1997. The interaction between cytoplasmic dynein and dynactin is required for fast axonal transport. *Proc. Natl. Acad. Sci. USA.* 94:12180–12185.
- Weiner, O.H., J. Murphy, G. Griffiths, M. Schleicher, and A.A. Noegel. 1993. The actin-binding protein comitin (p24) is a component of the Golgi apparatus. *J. Cell Biol.* 123:23–34.
- Welker, D.L., and K.L. Williams. 1980. Mitotic arrest and chromosome doubling using thiabendazole, cambendazole, nocodazole, and ben late in the slime mould *Dictyostelium discoideum*. *J. Gen. Microbiol.* 116:397–407.
- Wilkerson, C.G., S.M. King, A. Koutoulis, G.J. Pazour, and G.B. Witman. 1995. The 78,000 M(r) intermediate chain of *Chlamydomonas* outer arm dynein is a WD-repeat protein required for arm assembly. *J. Cell Biol.* 129:169–178.
- Wittmann, T., H. Boleti, C. Antony, E. Karsenti, and I. Vernos. 1998. Localization of the kinesin-like protein xklp2 to spindle poles requires a leucine zipper, a microtubule-associated protein, and dynein. *J. Cell Biol.* 143:673–685.
- Xiang, X., S.M. Beckwith, and N.R. Morris. 1994. Cytoplasmic dynein is involved in nuclear migration in *Aspergillus nidulans*. *Proc. Natl. Acad. Sci. USA.* 91:2100–2104.
- Yu, H., I. Toyoshima, E.R. Steuer, and M.P. Sheetz. 1992. Kinesin and cytoplasmic dynein binding to brain microsomes. *J. Biol. Chem.* 267:20457–20464.